Stress analysis of thick walled composite tubes under bending moment

S. Khadem Moshir[1]*, S.V. Hoa[2], and F. Shadmehri[3]
Concordia Center for Composites (CONCOM)
Department of Mechanical, Industrial and Aerospace Engineering
Concordia University[1,2,3]
Center for Research in Polymers and Composites (CREPEC)
Montreal, Quebec, Canada

* Corresponding author (s_hademm@encs.concordia.ca)

ABSTRACT

In this paper, the stress and failure analyses of composite thermoplastic Carbon/PEKK tubes are investigated. The application of these composites has been attracting interests for manufacturing the cross tubes in landing gear of helicopters. The tubes are manufactured by the automated fibre placement machine. Using the analytical theory elasticity of Lekhnitskii, the stress and failure of straight tubes subjected to three-points bending loading are investigated. In addition, the finite element method is applied and validated by the analytical solution. Both the finite element and analytical results are compared with the experimental data to figure out the capability of analytical method for determining the failure load of the tubes. The analytical method is useful in terms of time of computation with respect to the finite element solution.

KEYWORDS: *stress analysis, failure analysis, pure bending, thick composite tube*

1 INTRODUCTION

Having benefits over other materials in terms of light weight, high stiffness, high strength and good corrosion resistance, composite materials are being used more in many industries. One particular application of composites in the aerospace industry is the use of thermoplastic composite tubes as cross tubes for the landing gear in helicopters (ski type landing gears). It was shown that it may be possible to design and make thermoplastic composite tubes that exhibit similar performance as that of an aluminium tube with 30% lighter weight (Derisi 2008; Derisi et al. 2012; Derisi et al. 2010). These thermoplastic composite tubes have thick wall (about 12 mm thick) and containing many layers (100 to 200 layers). They are made by automated fiber placement and using carbon/PEKK thermoplastic composite materials. The results have been obtained using straight tubes and static loading conditions (three-points and four-points bending).

Some experimental and theoretical works have been carried out to study flexural behaviour of the composite tubes subjected to pure bending loads. Tarn and Wang (2001) applied an exact analytical solution to study extension, torsion, bending, anti-plane and in-plane shearing and pressuring of laminated composite tubes based on general expressions for the displacements of Lekhnitskii (Lekhnitskii et al. 1964) and also the plane strain assumption was used. They formulated the basic equations of anisotropic elasticity in cylindrical coordinate system into a state equation by a judicious arrangement of the displacement and stress variables. Xia et al. (2002) provided an exact solution based on classical laminate-plate theory for pure bending analysis of multi-layered filament-wound composite pipes based on Lekhnitskii's stress function. It is noted that the out-of-plane shear stress effects were not considered in their analysis. Saggar (2007) experimentally studied four-points bending of thin composite tubes and compared their data with classical lamination approach. Blom et al. (2010) tested pure bending of carbon-fiber reinforced composites cylinders including baseline laminate and circumferentially varying laminate stiffness. They also carried out a finite element analysis (FEA) of tubes in order to compare them with the experimental results. Arjomandi and Taheri (2012) employed finite element method (FEM) to study pure bending, nonlinear buckling and post-buckling of sandwich pipes. Menshykova and Guz (2014) investigated stress analysis of multi-layered thick-walled fiber reinforced composite straight pipes manufactured by filament winding process under bending loading. They used the axial stress relation of Lekhnitskii. Sun et al. (2014) carried out a stress analysis of hollow cylindrical structures including multiple anisotropic layers using stress functions proposed by Lekhnitskii. They also provided solutions for a homogenized composite cylinder with single-layer. Their solution is sufficient for stress analysis of thin-walled or moderately thick-walled hollow composite cylindrical structures. They compared the obtained results which were for composite tube with lay-up excepted for 0 or 90 winding angle degree of the layers by the FEM. Ahmad and Hoa (2016) obtained flexural stiffness of two-layered thick composite tubes by utilizing three dimensional theory of elasticity proposed by (Jolicoeur and Cardou 1994). They examined and compared theoretical results and experimental ones only for tubes with lay-up of [25/-25]. Akgun et al. (2017) employed differential quadrature method to investigate nonlinear static behaviour of laminated composite beams with hollow elliptical section subjected to three-point and end loading. The tube has oval and elliptic cross section which has adjusted parameters in the formulations (Lame curves). The nonlinearity is considered by applying Von-Karman strain displacement relations.

In the present work, an analytical method based on the theory elasticity of Lekhnitskii, which was developed by Zhang et al. (2014) for composite tubes which includes different lay-ups is used. The capability of the analytical method for stress and failure analysis of composite tubes is investigated.

2 SOLUTION PROCEDURE

A composite tube consisting of different cylindrical layers (N) is shown in Figure 1. The tube has elastic moduli E_1 and E_2 in fiber and transverse directions of each layer, respectively. The in-plane shear modulus and Poisson's ratios are G_{12}, G_{13}, ν_{12}, ν_{13} and the out-of-plane shear moduli and Poisson's ratio are G_{23} and ν_{23}. The tube with a winding angle of φ which is the angle between z axis and fiber direction is subjected to bending moments M_x and M_y. In the cylindrical coordinate system, r, θ and z are the radial, circumferential and longitudinal directions. The inside radius of each layer is denoted as b_n.

The fundamental equations of an analytical approach were provided by (Lekhnitskii et al. 1964) for the first time. He derived a set of partial differential equations for an isotropic single layered cylinder under axisymmetric loading.

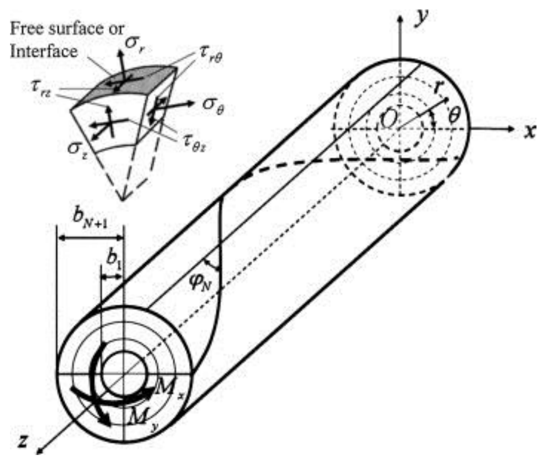

Figure 1: A composite tube subjected to pure bending (Zhang et al. 2014).

Following this approach, a coaxial hollow circular orthotropic cylinder subjected to combined bending, tensile and torsion loads was analysed analytically by (Jolicoeur and Cardou 1994) in order to obtain stresses, flexural stiffness as well as displacements. Two types of no slip and no friction conditions between layers were considered. Their formulation could not be used for tubes including 0 or 90 winding angle layers. (Zhang et al. 2014) provided a solution based on the formulations of (Jolicoeur and Cardou 1994) for tubes which contain 0 or 90 winding angle layers. In this solution, the tube is subjected to pure bending moment. In addition, in the FEM solution the tubes are under pure bending moment. Therefore, the effect of stress concentration due to the loading nose of the machine load in the three-points bending is not considered in the analytical solution. The stresses in the analytical method are as follows.

$$\sigma_r = \left(\kappa_x \sin(\theta) - \kappa_y \cos(\theta)\right)\left(\sum_{i=1}^{2} K_i r^{m_i-1} + \sum_{j=3}^{4} K_j^* g_j^* r^{m_j-1} + \mu_1 r\right) \quad (1)$$

$$\sigma_\theta = \left(\kappa_x \sin(\theta) - \kappa_y \cos(\theta)\right)\left(\sum_{i=1}^{2} K_i \left(m_i+1\right) r^{m_i-1} + \sum_{j=3}^{4} K_j^* g_j^* \left(m_j+1\right) r^{m_j-1} + 3\mu_1 r\right) \quad (2)$$

$$\sigma_z = \frac{1}{C_{33}}\left(\kappa_x r \sin(\theta) - \kappa_y r \cos(\theta) - C_{13}\sigma_r - C_{23}\sigma_\theta - C_{34}\tau_{\theta z}\right) \quad (3)$$

$$\tau_{r\theta} = \left(\kappa_x \cos(\theta) + \kappa_y \sin(\theta)\right)\left(-\sum_{i=1}^{2} K_i r^{m_i-1} + \sum_{j=3}^{4} K_j^* g_j^* r^{m_i-1} - \mu_1 r\right) \quad (4)$$

$$\tau_{rz} = \left(\kappa_x \cos(\theta) + \kappa_y \sin(\theta)\right)\left(\sum_{i=1}^{2} K_i g_i r^{m_i-1} + \sum_{j=3}^{4} K_j^* r^{m_j-1} + \mu_2 r\right) \quad (5)$$

$$\tau_{\theta z} = \left(\kappa_x \sin(\theta) - \kappa_y \cos(\theta)\right)\left(-\sum_{i=1}^{2} K_i g_i m_i r^{m_i-1} - \sum_{j=3}^{4} K_j^* m_j r^{m_j-1} - 2\bar{\mu}_2 r\right) \quad (6)$$

The variables and the further details of the above relations can be found in (Zhang et al. 2014).

The stress analysis of two tubes is done to figure out the correlation between the experimental and theoretical results.

3 FLEXURAL STIFFNESS, FAILURE AND STRESS ANALYSIS OF TUBE 1

A tube with lay-up sequence winding angle of $[(90^{\circ}_{10}/0^{\circ}_{10})_3/\pm45^{\circ}_{25}]$ and inner and outer diameters of 56 mm and 78 mm with the thickness ratio of (0.141) and has span of 890 mm is subjected to three-points bending loading. The force-longitudinal strain at the mid-span and bottom of tube is shown in the Figure 2. The slope of the diagram leads to the flexural stiffness of the tube. It can be seen that while the analytical solution and the FEM predict the flexural stiffness of the tube 22.1% and 20.1% more than the experiment does (Derisi et al. 2012), respectively.

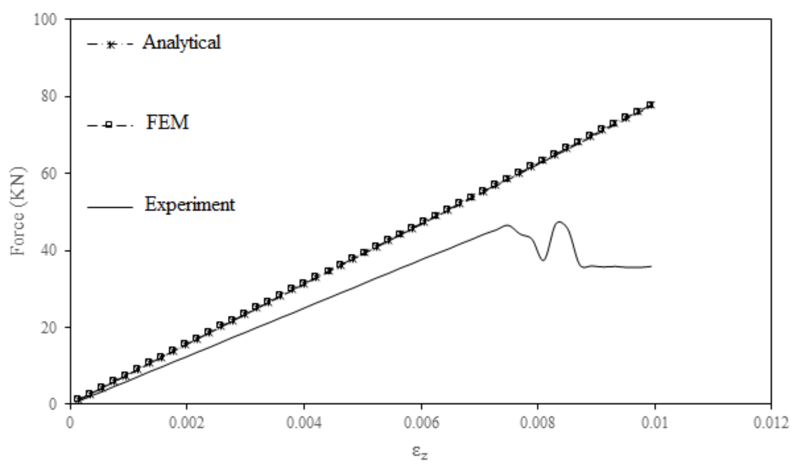

Figure 2: Change of longitudinal strain (mid-length and bottom surface) with applied force for three-point bending of tube 1, $[(90^{\circ}_{10}/0^{\circ}_{10})_3/\pm45^{\circ}_{25}]$.

According to the Tsai-Wu failure criterion, the first ply failure is occurred at the moment of M_x=17.3 KN.m. The inter-laminar radial stress distribution at the first ply-failure moment is demonstrated in Figure 3 (a). It can be seen that at the 90° and 0° layers the inter-laminar radial stress has stepwise change and it has linear variation at the $\pm45^{\circ}$ layers. The distribution of circumferential stress through the thickness is shown in the Figure 3 (b). The longitudinal stress (Figure 4 (a)) is also has fluctuations as the circumferential stress. The tube does not carry the out-of-plane shear stress $\tau_{\theta z}$ at the 90° and 0° layers, however, it has periodical change at the $\pm45^{\circ}$ layers as shown in Figure 4 (b).

The maximum carried moment of the tube 1 according to the Tsai-Wu, maximum stress criterion and experiment is reported in the Table 1. It can be observed there is a large difference between the experimental results and the theoretical ones. In the test, the tube was subjected to three-points bending loading. This failure (V-type) in the test can be due to the effect of stress concentration of the loading nose although a pad at the loading nose has been used to reduce this effect.

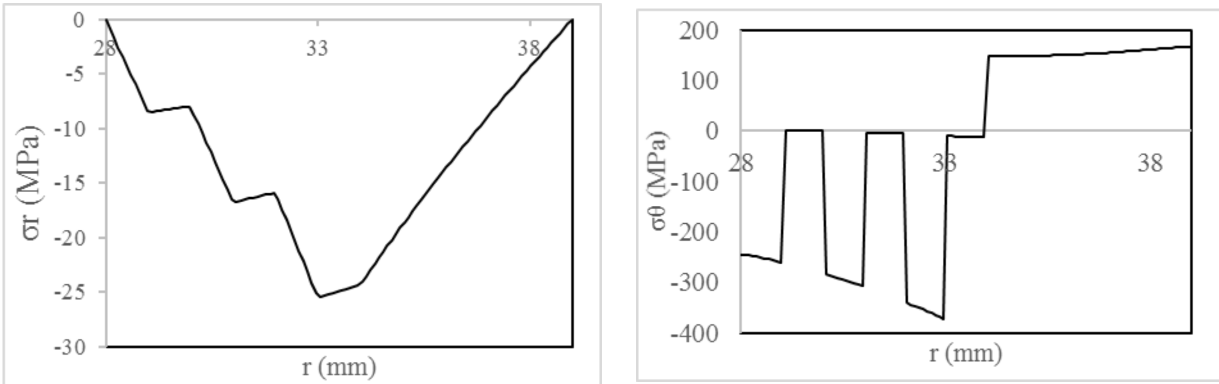

(a) (b)

Figure 3: The distribution of a) inter-laminar radial stress b) circumferential stress, through the thickness of the tube 1 at $\theta = 90^{\circ}$, at first ply failure based on Tsai-Wu criterion (M_x=17.3 KN.m.).

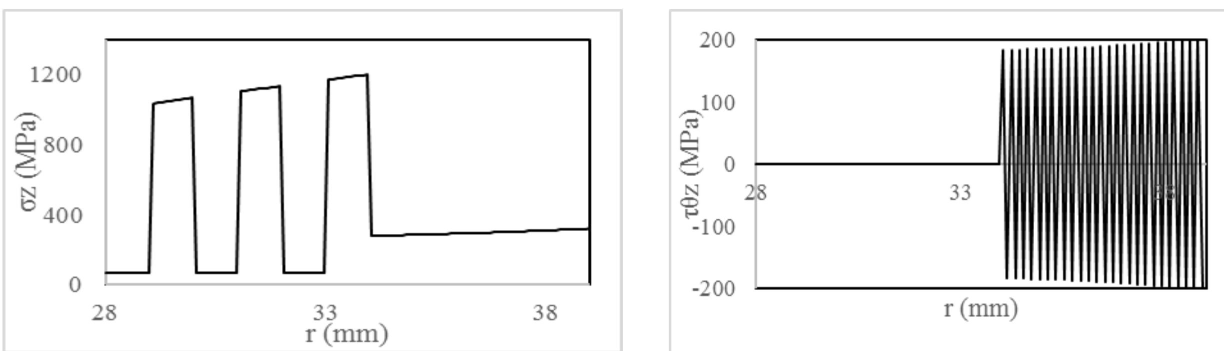

(a) (b)

Figure 4: The distribution of a) the longitudinal stress b) the out-of-plane shear stress through the thickness of the tube 2 at $\theta = 90^{\circ}$, at first ply failure based on Tsai-Wu criterion (M_x=17.3 KN.m.).

Table 1 Maximum bending moment (in KN.m) of the tube 1 until its first ply failure.

Method	Maximum stress	Tsai-Wu
Analytical	20	17.3
FEM	20	17.3
Experiment	10.0	

Figure 5: Fracture of tube 1 due to stress concentration at the loading nose, (Derisi 2008).

4 FAILURE AND FLEXURAL STIFFNESS OF TUBE 2

The second tube has the lay-up sequence winding angle of $[90^{\circ}_{30} / \pm25^{\circ}_{45} / 90^{\circ}_{5} / \pm30^{\circ}_{20} / 90^{\circ}_{5} / \pm45^{\circ}_{20}]$ with the inner and outer diameters of diameter of 56 mm and 98 mm with the thickness ratio of (0.428) and the span of 890 mm. The tube is subjected to three-points bending loading test. The force-longitudinal strain at the mid-span and bottom surface of the tube in the Figure 6 shows that the percentage difference in the flexural stiffness between the analytical as well as the FEM with respect to the experiment (Derisi et al. 2012) is 5.6 and 5.9, respectively.

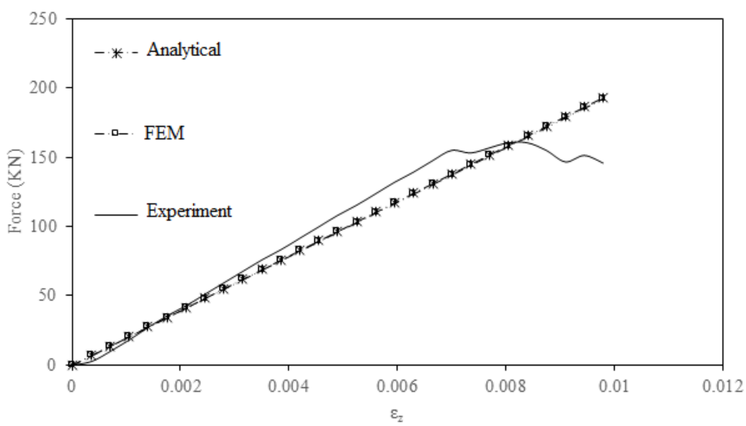

Figure 6: Change of longitudinal strain (mid-length and bottom surface) with applied force for three-point bending of tube 2, $[90^{\circ}_{30} / \pm25^{\circ}_{45} / 90^{\circ}_{5} / \pm30^{\circ}_{20} / 90^{\circ}_{5} / \pm45^{\circ}_{20}]$.

The maximum bending moment at the first ply failure is shown in Table 2. It is seen that based on the maximum stress criterion the first ply failure occurs at outermost 90°_{5} layers at $\theta = 90^{\circ}$ with the transverse matrix cracking at M= 47 KN.m. According to Tsai-Wu criterion, the maximum bending moment carried by tube 2 until its first ply failure obtained by analytical and FE methods is 35 KN.m. This bending moment is also reported through experimental study

(Derisi et al. 2012) which is 36.7 KN.m. Moreover, a comparison between the failure moments obtained by two failure criteria shows that the Tsai-Wu has better prediction than the maximum stress criterion.

Table 2 Maximum bending moment (in KN.m) of the tube 3 until its first ply failure.

Method	Maximum stress	Tsai-Wu
Analytical	47	35
FEM	47	35
Experiment	36.7	

Unlike the tube 1, this tube does not have V-type failure and it remains curved at the failure load. In addition, there is a good agreement between the Tsai-Wu failure criterion and the experiment. It means that the stress concentration at the loading nose does not have significant effect on the failure of this tube.

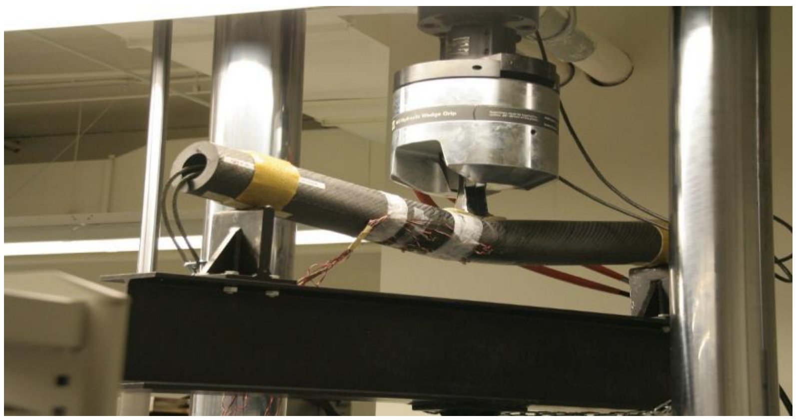

Figure 7: Failure of tube 3, (Derisi 2008).

Discussion: There are a few assumptions made in this paper. First is the use of the analytical method, and FEM method, developed for pure bending of beam, and compare their results with experimental results done on beams under three-points bending. In three-points bending, there are shear loads and shear stresses. The effect of these shears may influence the results. Full 3D finite element solutions for the beams under 3-point bending need to be carried out to see the effect. Secondly, experimental tube 1 suffers from stress concentration due to the loading and support conditions. As such, comparison with analytical method where no stress concentration is considered may not be fair. More tubes will be tested in the near future to provide better information.

5 CONCLUSION

The stress and failure analyses of composite tubes with different lay-ups are investigated to find the correlation between the analytical method proposed by Zhang et al. (2014), FEM and experimental results. The following conclusions can be drawn:

- The failure moment of the analytical method agrees well with the FEM for tubes subjected to pure bending moment.
- There is a good agreement between the experimental results and the analytical method for tube 2. It means that the effect of stress concentration does not have substantial effect on the failure of this tube.

REFERENCES

Ahmad, M. G., and Hoa, S. (2016). Flexural stiffness of thick walled composite tubes. *Composite Structures*, 149, 125-133.

Akgun, G., Algul, I., and Kurtaran, H. (2017). "Nonlinear Static Analysis of Laminated Composite Hollow Beams with Super-Elliptic Cross-Sections." *World Academy of Science, Engineering and Technology, International Journal of Mechanical, Aerospace, Industrial, Mechatronic and Manufacturing Engineering*, 11(8), 1460-1465.

Arjomandi, K., and Taheri, F. (2012). "Bending capacity of sandwich pipes." *Ocean Engineering*, 48, 17-31.

Blom, A., Stickler, P., Rassaian, M., and Gürdal, Z. Bending Test of a Variable-Stiffness Fiber Reinforced Composite Cylinder. *Proc., 51st AIAA/ASME/ASCE/AHS/ASC Structures, Structural Dynamics, and Materials Conference 18th AIAA/ASME/AHS Adaptive Structures Conference 12th*, 2600.

Chan, W. S., and Demirhan, K. C. (2000). A Simple Closed-Form Solution of Bending Stiffness for Laminated Composite Tubes. *Journal of Reinforced Plastics and Composites,* 19(4), 278-291.

Derisi, B. (2008). *Development of thermoplastic composite tubes for large deformation*, Concordia University, Montral.

Derisi, B., Hoa, S., and Hojjati, M. (2012). "Similitude study on bending stiffness and behavior of composite tubes." *Journal of Composite Materials*, 46(21), 2695-2710.

Derisi, B., Suong, H., Duosheng, X., Hojjati, M., and Fews, R. (2010). "Composite Tube Exhibiting Large Deformation under Bending." *Journal of Composite Materials*, 44(16), 2005-2020.

Jolicoeur, C., and Cardou, A. (1994). Analytical solution for bending of coaxial orthotropic cylinders. *Journal of engineering mechanics*, 120(12), 2556-2574.

Jonnalagadda, A., Sawant, A., Rohde, S., Sankar, B., and Ifju, P. (2015). An analytical model for composite tubes with bend–twist coupling. *Composite Structures*, 131, 578-584.

Lekhnitskii, S., Fern, P., Brandstatter, J. J., and Dill, E. (1964). Theory of elasticity of an anisotropic elastic body. *Physics Today*, 17, 84.

Menshykova, M., and Guz, I. A. (2014). Stress analysis of layered thick-walled composite pipes subjected to bending loading. *International Journal of Mechanical Sciences*, 88, 289-299.

Saggar, P. (2007). Experimental study of laminated composite tubes under bending."

STOCKWELL, A., and COOPER, P. Collapse of composite tubes under end moments." *Proc., 33rd Structures, Structural Dynamics and Materials Conference*, 2389.

Sun, X., Tan, V., Chen, Y., Tan, L., Jaiman, R., and Tay, T. (2014). Stress analysis of multi-layered hollow anisotropic composite cylindrical structures using the homogenization method. *Acta Mechanica*, 225(6), 1649-1672.

Tarn, J.-Q., and Wang, Y.-M. (2001). Laminated composite tubes under extension, torsion, bending, shearing and pressuring: a state space approach. *International Journal of Solids and Structures*, 38(50-51), 9053-9075.

Xia, M., Takayanagi, H., and Kemmochi, K. (2002). Bending behavior of filament-wound fiber-reinforced sandwich pipes. *Composite structures*, 56(2), 201-210.

Zhang, C., Hoa, S. V., and Liu, P. (2014). A method to analyze the pure bending of tubes of cylindrically anisotropic layers with arbitrary angles including 0 or 90. *Composite Structures*, 109, 57-67.